

Spin squeezing can only improve clocks with small atom number

Marius Schulte,¹ Christian Lisdat,² Piet O. Schmidt,^{2,3} Uwe Sterr,² and Klemens Hammerer¹

¹*Institute for Theoretical Physics and Institute for Gravitational Physics (Albert-Einstein-Institute), Leibniz University Hannover, Appelstrasse 2, 30167 Hannover, Germany*

²*Physikalisch-Technische Bundesanstalt (PTB), Bundesallee 100, 38116 Braunschweig, Germany*

³*Institute for Quantum Optics, Leibniz University Hannover, Welfengarten 1, 30167 Hannover, Germany*

(Dated: July 7, 2022)

We show that the stability of an optical atomic clock can only be improved by spin squeezed states for ensembles below a critical particle number. This limitation results from a trade-off between measurement noise and instabilities due to limited laser coherence. Our results apply to the case of cyclic Ramsey interrogations on a single atomic ensemble with dead time between each measurement. The combination of analytical models for projection noise, dead time noise (Dick effect) and laser phase noise allows quantitative predictions of the critical particle number and the optimal clock stability for a given dead time and laser noise. Our analytical predictions are confirmed by numerical simulations of the closed servo loop of an optical atomic clock.

In recent years, atomic clocks based on optical transitions [1] have achieved unprecedented levels in accuracy and stability as frequency references [2–5]. Apart from a redefinition of the SI second, this also facilitates new tests of physics beyond the Standard Model [6–8] and opens up the field of relativistic geodesy [9–11]. For these applications, high clock stability is vital in order to reach a given frequency uncertainty in the shortest possible time. Accordingly, approaches from quantum metrology [12] are being pursued which promise to achieve an improvement through the use of entangled atoms. In particular, spin squeezed states [13–15] received much attention due to their practicability and noise resilience [12, 16]. Spin squeezed states can be generated with trapped ions [17–19] and in cold atomic gases [20–23], and have already been used in proof-of-principle experiments to demonstrate a reduction of quantum projection noise (QPN) in measurements of small phases on microwave transitions [24–27]. The realization of such tailored entangled states on optical clock transitions is a major challenge for experiment [27, 28] and theory [29–34].

In view of these advances, it is important to note that under practical conditions, optical atomic clocks are not exclusively limited by QPN. Indeed, the operating point of a clock at which maximum stability is achieved is determined by a balance of QPN and other noise processes, such as laser phase noise and dead time effects [35–38]. In this letter we assess the prospects for improving the stability of optical atomic clocks using spin squeezing under these conditions. Our main result is that at a given level of dead time and laser phase noise, spin squeezing can only offer an advantage for atomic numbers below a certain critical number of clock atoms. For state-of-the-art high-quality clock lasers, this critical atomic number is smaller than the size that can realistically be reached in optical lattice clocks without being limited by density effects. Thus, in lattice clocks spin squeezing can only provide an advantage with significant improvements in dead time and phase noise of next gener-

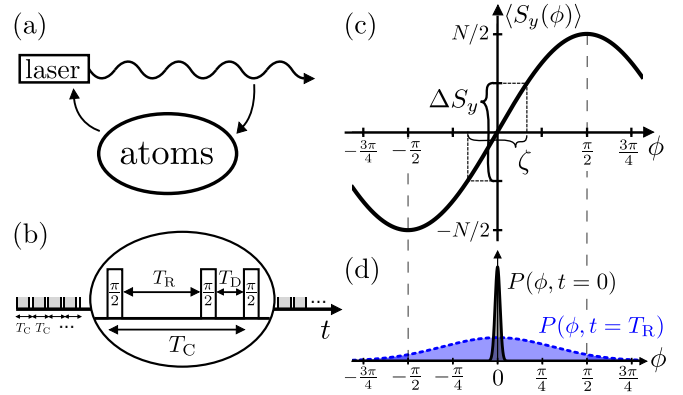


FIG. 1. (a) Measurement and feedback loop to stabilize the laser frequency to an atomic transition. (b) Periodic measurements with Ramsey time T_R and dead time T_D in each cycle of total time T_C lead to increased instability from the Dick effect. (c) Quantum projection noise ΔS_y limits the clock stability for short interrogation times but can be decreased with squeezed states thus reducing the inferred phase uncertainty ζ . (d) For longer T_R the distribution of phases broadens substantially due to the laser's decoherence. Inefficient feedback for phases outside the $[-\frac{\pi}{2}, \frac{\pi}{2}]$ interval gives the coherence time limit.

ation clock lasers. In contrast, in atomic clocks based on platforms whose atomic number cannot be easily scaled, such as ion traps or tweezer arrays [39–42], spin squeezing can offer a relevant advantage. We would like to stress that this limitation applies to single atomic clocks with conventional (Ramsey) interrogation sequences with squeezed input states. The limitation could be avoided with schemes achieving dead-time-free interrogation or overcoming laser phase noise [43–49]. The potential gain from entanglement should then be assessed by an appropriate analysis, incorporating the tradeoffs discussed here. In the following, we will first describe our main result more quantitatively, then present the details of our description and further explain implications of our key

findings.

In optical atomic clocks a laser of very high but finite coherence time is stabilized by a control loop to an atomic transition of frequency ν_0 , see Fig. 1(a). The laser frequency is compared to the atomic transition in a sequence of interrogation cycles, each of duration T_C . We consider here Ramsey interrogations with interrogation time T_R , and cycles with a dead time $T_D = T_C - T_R$, see Fig. 1(b). At the end of an interrogation cycle, the collective atomic spin is measured along a projection, which we take as S_y , providing information about the deviation of the laser from the atomic transition frequency, see Fig. 1(c). The measurement result is converted into an error signal that is used to correct the laser frequency. The clock instability achieved in this way after averaging over a time $\tau \gg T_C$ is measured in terms of the Allan deviation σ_y for fractional frequency fluctuations [1].

For an atomic clock whose stability is exclusively limited by the QPN of the spin measurements ΔS_y , the Allan deviation would be

$$\sigma_{\text{QPN}}(\tau) = \frac{1}{2\pi\nu_0 T_R} \sqrt{\frac{T_C}{\tau}} \zeta \quad (1)$$

with the phase uncertainty $\zeta = \Delta S_y / \langle S_x \rangle$, cf. Fig. 1(c). This is related to the Wineland spin squeezing parameter ξ by $\xi = \sqrt{N}\zeta$. For uncorrelated atoms with mean spin polarization along $\langle S_x \rangle$ the phase uncertainty scales with the number of atoms N as $1/\sqrt{N}$, the standard quantum limit. Correlated states of atoms can optimally change this scaling up to $1/N$ [12]. In particular spin squeezed states can reduce the QPN while maintaining a strong spin polarization, thus lowering ζ and ultimately σ_{QPN} .

As Eq. (1) suggests, the stability can also be improved by increasing the interrogation time T_R , provided the QPN still remains the dominant noise process. Obviously, it will be beneficial to increase T_R to a point where this is no longer the case, and the QPN is reduced to a level where other processes contributing to the clock instability become comparable. Which other noise processes become relevant first depends on the type of atomic clock. For the extremely narrow-band transitions that can be used in optical atomic clocks it is the finite coherence time of the clock laser rather than that of the atoms that is the limiting factor. Laser phase noise affects clock stability in two ways: Firstly, by phase diffusion during dead time (see Fig. 1(b)), the so-called Dick effect [50] whose contribution to the Allan deviation σ_{Dick} is well known and summarized below. Second, by phase diffusion during the interrogation, causing the distribution of the phase prior to the measurement to become wider. When the Ramsey dark time T_R becomes comparable to the laser coherence time the differential phase noise between laser and atomic reference can exceed the invertible domain of the Ramsey signal and thus no unambiguous estimate based on the measurement result is possible, as illustrated in Fig. 1(d). At this point, the feedback

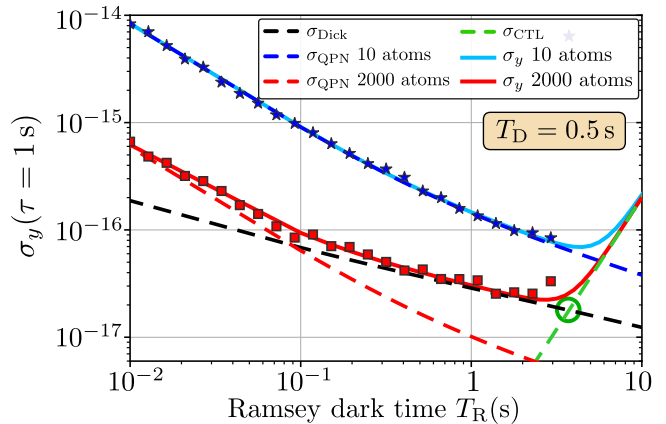


FIG. 2. Allan deviation of an atomic clock with $T_D = 0.5$ s dead time for $\tau = 1$ s of averaging time as a function of Ramsey dark time T_R . Solid lines are instabilities from the full noise model, Eq. (2), with $N = 10$ (blue) and $N = 2000$ (red) uncorrelated clock atoms. Dashed lines show the three contributing noise processes: QPN (blue and red), CTL (green), and the Dick noise (black) for ultra-stable clock lasers [53]. Symbols are numerical simulations of the closed feedback loop in agreement with the analytic model until the onset of fringe-hops leads to a sudden, strong increase in instability.

loop becomes ineffective, compromising stability in two ways: First, the finite laser coherence time contributes to the Allan deviation in the form of an additional diffusion process, which we refer to in the following as the laser coherence time limit (CTL). Building on previous work by Leroux et al. [36] and André et al. [51, 52], we develop below a detailed stochastic model of the CTL from which we can infer the continuous contribution to the Allan deviation σ_{CTL} . Second, laser phase noise can also result in an abrupt loss of clock stability when the stabilization passes to an adjacent fringe, causing the clock to run permanently wrong. We will show that the resulting limitation of the Ramsey time can be understood quantitatively in the framework of our stochastic model as a first escape time, giving good agreement with previous phenomenological estimates [36]. We find that in the regime of a good atomic clock (long laser coherence time and small dead time) the diffusive process σ_{CTL} constitutes the more stringent limitation for the Ramsey interrogation, so that we concentrate on the discussion of this effect for the time being.

Incorporating these additional effects, the optimal operating point of the control loop has to be determined from a tradeoff between QPN, Dick effect, and CTL, by minimizing the combined instability

$$\sigma_y(\tau) = \sqrt{\sigma_{\text{QPN}}^2(\tau) + \sigma_{\text{Dick}}^2(\tau) + \sigma_{\text{CTL}}^2(\tau)}. \quad (2)$$

Without already going into the specific functional dependence of σ_{Dick} and σ_{CTL} on the parameters that characterize the atomic clock, we can highlight the most im-

portant features, most of which are very intuitive to understand: Just as the QPN, the Dick noise is monotonically decreasing with longer Ramsey time as the relative weight of the dead time T_D goes down. However the CTL will increase with T_R , as explained above. In contrast to QPN, both Dick and CTL noise do not depend on the size of the atomic ensemble N . This should be clear for the Dick effect, which is determined by the laser noise, T_D and T_R only. The fact that the CTL does not depend on N is not so obvious, and will be shown below. These scalings are visible in Fig. 2 which shows the combined Allan deviation, Eq. (2), and all three contributing noise processes versus Ramsey time for a small ensemble ($N = 10$, blue solid line) and a larger ensemble of atoms ($N = 2000$, red solid line) in a coherent spin state. Solid lines in Fig. 2 correspond to the analytical models, symbols show the results of numerical simulations of the closed feedback loop (see appendix IV) in excellent agreement with the theoretical curves.

In view of Fig. 2 (which concerns uncorrelated atoms in coherent spin states) several observations can be made: First, the instability will attain a minimum for a certain interrogation time. We assume in the following that the clock can operate at this optimal time without running into technical problems such as optical path length fluctuations and others. Second, important distinctions can be made based on the particle number N . For small ensembles, where QPN dominates over the Dick effect, the minimal instability is set by a tradeoff between QPN and the CTL (cf. blue line). This minimum depends on N . However for large ensembles, where the Dick effect dominates over QPN, the minimal instability is set by a tradeoff between the Dick effect and the CTL (cf. red line). This minimum does not depend on N and is determined only by laser noise and dead time [54]. In particular there exists a time T_R^* where both processes contribute equally, i.e. $\sigma_{\text{Dick}}|_{T_R^*} = \sigma_{\text{CTL}}|_{T_R^*}$. The instability $\sigma_{\min} = \sigma_{\text{Dick}}|_{T_R^*} \equiv \sigma_{\text{CTL}}|_{T_R^*}$ at this point provides a lower bound to the overall instability, indicated by the green circle in Fig. 2. We now compare Allan deviations at $\tau = 1$ s. Figure 3(a) shows σ_{\min} as a function of T_D for three types of lasers: a state of the art high quality clock laser [53], limited by flicker frequency noise at an Allan deviation $\sigma_{\text{FF}} = 4.9 \times 10^{-17}$, future generation clock lasers with projected improved noise spectra such that $\sigma_{\text{FF}} = 10^{-17}$ or 3×10^{-18} , and a laser for transportable atomic clocks at $\sigma_{\text{FF}} = 10^{-16}$. An almost universal behaviour emerges, as shown in the inset of Fig. 3(a), on re-scaling T_D and σ_{\min} by a laser coherence time Z , which we define as $\sigma_{\text{LO}}(Z)2\pi\nu_0Z = 1$ rad following [36]. Deviations from this scaling behaviour for $T_D \lesssim 5 \times 10^{-2}$ s are likely due to the complicated dependence of σ_{Dick} on the duty factor T_R/T_C . [55] Ultimately, since the QPN can be reduced by increasing N , this implies that there is a certain critical number of particles

N_{\min} which is required to achieve the minimal instability, given T_D and the laser stability. (At this particle number QPN will dive below the green circle in Fig. 2.) We evaluate this as $N_{\min} = \min_N \{\sigma_{\text{QPN}}|_{N,T_R^*} \leq \sigma_{\min}\}$. To assess whether N_{\min} reaches the minimal instability we need to additionally compare T_R^* with the Ramsey time T_{FH} at which fringe-hops appear with probability 1 per total number of clock cycles ($\sim 10^6$ in the numerical simulations performed here). We are able to determine T_{FH} by extending the stochastic differential equation formalism (see appendix III) to an equivalent Fokker-Planck equation. From this, a mean first escape time for the phase of the stabilized laser can be calculated. We find that fringe-hops occur when the escape time from the interval $[-\pi, \pi]$ reaches the total number of clock cycles. Our results are in agreement with a previous phenomenological guide $T_{\text{FH}} = (0.4 - 0.15N^{-1/3})Z$ [36]. In many cases the minimal instability can be reached before being limited by fringe-hops, i.e. $T_R^* < T_{\text{FH}}$, with exceptions only at short laser coherence times and long dead times as shown in appendix III.

So far, all statements referred to uncorrelated atoms. Provided we perform Ramsey interrogation of a single ensemble of atoms, under which conditions can the clock stability be improved by employing squeezed spin states? First, it is clear that the limitation due to dead time in form of the Dick effect will not be reduced by atomic correlations. On the contrary, additional preparation time may even lead to an increase in instability there. Strongly squeezed or other highly entangled states will result in a more restrictive CTL and are unfavorable also for several other reasons (stronger decoherence, unfeasible requirements on measurements etc.). Therefore we consider here only moderately squeezed states which maintain the fringe width and contrast, leaving the CTL largely at the level of coherent states [51]. Specifically, we assume states generated via the unitary one-axis twisting interaction $e^{-i(\mu/2)S_z^2}$ for which the squeezing strength, $\mu \approx 1.1 N^{-2/3}$, was independently optimized to give the lowest instability at each N in the dead time free case. From the discussion above we conclude that an increased stability using spin squeezed states is only possible in small ensembles with particle numbers $N < N_{\min}^{(\text{CSS})}$ for a given T_D and laser noise. The instability can be reduced at most down to the limit set by the Dick effect and CTL. However the required minimal particle number will be lower than for coherent spin states, $N_{\min}^{(\text{SSS})} < N_{\min}^{(\text{CSS})}$. We show N_{\min} for uncorrelated particles (full lines) and squeezed states (dashed) versus T_D in Fig. 3(b). This shows significantly reduced N_{\min} for squeezed states at small dead times and highlights how improvements in the laser coherence time would make larger ensembles or squeezed states in lattice clocks eventually necessary. Figure 3(c) shows the instability versus particle number for various levels of dead time with and without spin

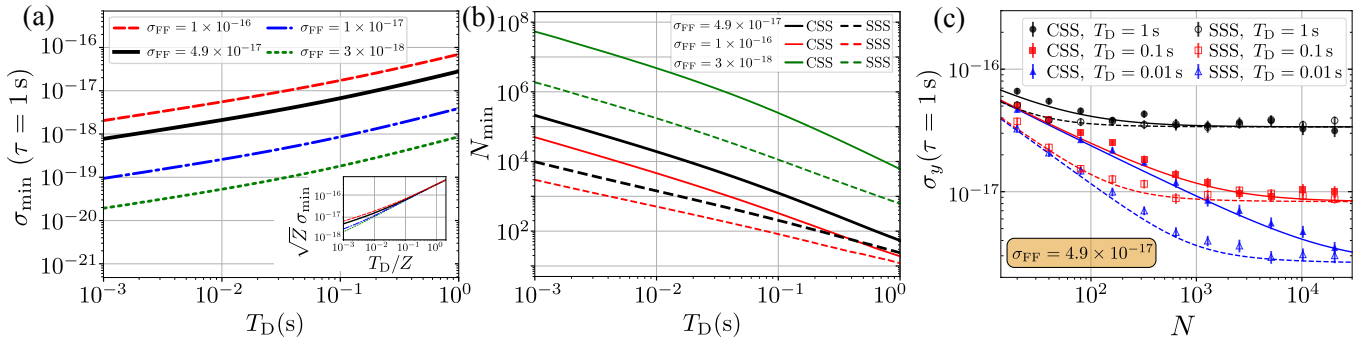


FIG. 3. (a) Ensemble size independent stability bound σ_{\min} as a function of dead time and with different laser phase noise, quantified by its flicker frequency Allan deviation. Inset: Normalizing by the laser coherence time Z reveals equal scaling at longer dead times. (b) Minimal required particle number for reaching the stability limit with uncorrelated particles (full lines) or spin squeezed initial states (dashed lines). (c) Particle number scaling towards the lower bound σ_{\min} for $T_D = 1$ s, 0.1 s, 0.01 s. The stability for each N is optimized over the Ramsey time. Compared are uncorrelated atoms in a coherent spin state (CSS, full lines and symbols) and squeezed spin states (SSS, dashed lines and empty symbols).

squeezing. This illustrates the crossover between the two regimes with N below and above N_{\min} . Additionally, it shows that N_{\min} cannot represent a sharp threshold value, but rather should be seen in relation to the asymptotic approach to σ_{\min} . We infer that, especially for large ensembles, a gain in stability can be expected only for quite challenging levels of dead time. These conclusions also imply that the asymptotic (large N) scaling of phase sensitivity in quantum metrology is largely irrelevant.

In the last part of this article we will provide more technical background for the description of the Dick effect and the CTL. The Dick noise, for Ramsey interrogation with infinitely short $\pi/2$ pulses, is [50]

$$\sigma_{\text{Dick}}^2(\tau) = \frac{1}{\tau} \frac{T_{\text{C}}^2}{T_{\text{R}}^2} \sum_{k=1}^{\infty} S_y(k/T_{\text{C}}) \frac{\sin^2(\pi k T_{\text{R}}/T_{\text{C}})}{\pi^2 k^2} \quad (3)$$

where $S_y(f)$ is the laser's single-sided fractional frequency noise power spectral density. We assume $S_y(f) = \sum_{k=-2}^0 h_k f^k$ with $h_{-2} = 2.4 \times 10^{-37}$ Hz, $h_{-1} = 1.7 \times 10^{-33}$, $h_0 = 1.3 \times 10^{-33}$ Hz $^{-1}$ for a clock laser which is mainly limited by flicker frequency noise at $\sigma_{\text{FF}} = 4.9 \times 10^{-17}$ [53]. To represent lasers of varying quality the entire spectral density is scaled. When necessary we use the frequency $\nu_0 \approx 429.228$ THz of ^{87}Sr for calculations. For modelling the CTL we build on [36, 51, 52], and infer the instability due to measurement noise and ineffective feedback based on a stochastic differential equation (SDE). The SDE describes the evolution of the stabilized laser frequency, driven by noise from the free-running laser but cyclically corrected using information from the measurements, including projection noise. We review the approach in appendix III, along with new results regarding the necessary feedback and ways to include fringe-hops. A perturbative solution of the SDE in powers of the laser phase variance then allows us to describe the effects of finite laser coherence in lowest order.

The CTL results as a contribution in third order of the laser phase variance. If the free-running laser stability is dominated by power-law noise (i.e. $\sigma_{\text{LO}}(\tau) \propto \tau^\gamma$ with $\gamma = -1, 0, 1$ corresponding to white, flicker and random walk frequency noise respectively) the laser phase variance $V_\phi = \chi(\gamma) (T_{\text{R}}/Z)^{2+\gamma}$ scales at specific powers of T_{R}/Z and with $\chi(\gamma)$ of order unity. As a main result, the SDE gives $\sigma_{\text{eff}}^2(\tau) = V_{\text{eff}} T_{\text{C}} / (2\pi\nu_0 T_{\text{R}} \sqrt{\tau})^2$. The effective measurement variance is [52] $V_{\text{eff}} = V_0 + V_1 + \mathcal{O}(V_\phi^4)$ with

$$V_0 = \frac{\Delta S_y^2}{\langle S_x \rangle^2} + \frac{\Delta S_x^2}{\langle S_x \rangle^2} V_\phi + \frac{3(1-c)^2}{8} \frac{\Delta S_y^2}{\langle S_x \rangle^2} V_\phi^2 \quad (4)$$

and $V_1 = (1/6 - c/2 + 4c^2/9)V_\phi^3$. Here $c = g\langle S_x \rangle/N$ and g is the gain factor of an integrating servo in the feedback loop, see appendix III. This holds for Ramsey interrogation with weakly squeezed initial states, where measurement statistics are approximated by Gaussian distributions (see appendix I for expectation values and variances). As above, σ_{eff}^2 can be separated in the following way: All terms in V_0 contain spin variances and reduces to $V_0 = \zeta^2$ in the limit $T_{\text{R}} \ll Z$, reproducing the QPN, so $\sigma_{\text{QPN}}^2(\tau) = V_0 T_{\text{C}} / (2\pi\nu_0 T_{\text{R}} \sqrt{\tau})^2$. The CTL is $\sigma_{\text{CTL}}^2(\tau) = V_1 T_{\text{C}} / (2\pi\nu_0 T_{\text{R}} \sqrt{\tau})^2$ as V_1 is the first order with an N -independent contribution. This term results conceptually from the lowest order (cubic) non-linearity of the sinusoidal Ramsey signal.

In conclusion, we would like to emphasize that the theoretical and experimental progress in manipulating the QPN in quantum metrological measurements with entangled states represents an important and exciting challenge. In the context of atomic clocks, however, a reduction in the QPN does not automatically mean an improvement in statistical uncertainty. A possible gain through entangled states therefore requires an evaluation that is detailed to the specific conditions of an atomic clock. For GHZ states in microwave clocks, which are

limited by QPN and atomic decoherence, this was already done quite some time ago in [35]. Here, we have done the same for optical atomic clocks and squeezed states. Although we showed that current improvements are limited to small systems only, our results also indicate that after challenging improvements in laser stability and dead time spin squeezing will become relevant for optical lattice clocks as well. In order to promote the use of entanglement in optical clocks, a number of further aspects should be considered in a similar way: Excess anti-squeezing due to imperfect state preparation has been considered in [37], and shown to reduce clock stability for white laser noise. It would be desirable to incorporate excess anti-squeezing to our model which deals with realistic colored laser noise. To what extent other measurement methods besides Ramsey interrogation are subject to similar restrictions or in which cases they can be circumvented remains open. Rabi interrogation is not expected to give improvements over the limits presented here due to its increased QPN and enhanced Dick effect [56], even though it allows for longer interrogations than Ramsey protocols. The limitations described here may be overcome with more sophisticated clock architectures: The laser coherence limit can be tackled with adaptive measurement schemes [57] or cascaded systems with multiple ensembles of atoms [43–45]. Dead time free laser stabilization, basically eliminating the Dick effect, was constructed by anti-synchronized interrogations of two atomic clocks [48]. Conceptually different approaches that may evade the presented limitations are based on continuously tracking the atomic phase via weak measurements [58–60].

We acknowledge valuable contributions from I. D. Leroux in initiating the numerical simulation of atomic clocks applied here. This work is supported by the DFG through CRC 1227 DQ-mat projects A05, A06, B02, B03 and the cluster of excellence ‘Quantum Frontiers’. P. O. Schmidt and U. Sterr acknowledge funding from EMPIR under project USOQS.

-
- [1] A. D. Ludlow, M. M. Boyd, J. Ye, E. Peik, and P. O. Schmidt, “Optical atomic clocks,” *Rev. Mod. Phys.*, vol. 87, pp. 637–701, Jun 2015.
- [2] T. Nicholson *et al.*, “Systematic evaluation of an atomic clock at 2×10^{-18} total uncertainty,” *Nature communications*, vol. 6, p. 6896, 2015.
- [3] W. F. McGrew *et al.*, “Towards the optical second: verifying optical clocks at the SI limit,” *Optica*, vol. 6, pp. 448–454, Apr 2019.
- [4] N. Huntemann, C. Sanner, B. Lipphardt, C. Tamm, and E. Peik, “Single-ion atomic clock with 3×10^{-18} systematic uncertainty,” *Phys. Rev. Lett.*, vol. 116, p. 063001, Feb 2016.
- [5] S. M. Brewer, J.-S. Chen, A. M. Hankin, E. R. Clements, C. W. Chou, D. J. Wineland, D. B. Hume, and D. R. Leibrandt, “ $^{27}\text{Al}^+$ quantum-logic clock with a systematic uncertainty below 10^{-18} ,” *Phys. Rev. Lett.*, vol. 123, p. 033201, Jul 2019.
- [6] P. Delva *et al.*, “Test of special relativity using a fiber network of optical clocks,” *Phys. Rev. Lett.*, vol. 118, p. 221102, Jun 2017.
- [7] C. Sanner, N. Huntemann, R. Lange, C. Tamm, E. Peik, M. S. Safranova, and S. G. Porsev, “Optical clock comparison for Lorentz symmetry testing,” *Nature*, vol. 567, pp. 204–208, Mar 2019.
- [8] B. M. Roberts *et al.*, “Search for transient variations of the fine structure constant and dark matter using fiber-linked optical atomic clocks,” *arXiv e-prints*, p. arXiv:1907.02661, Jul 2019.
- [9] C. Lisdat *et al.*, “A clock network for geodesy and fundamental science,” *Nature Communications*, vol. 7, Aug 2016.
- [10] J. Grotti *et al.*, “Geodesy and metrology with a transportable optical clock,” *Nature Physics*, vol. 14, pp. 437–441, Feb 2018.
- [11] T. Mehlstäubler, G. Grosche, C. Lisdat, P. O. Schmidt, and H. Denker, “Atomic clocks for geodesy,” *Reports on Progress in Physics*, vol. 81, p. 064401, Apr 2018.
- [12] L. Pezzè, A. Smerzi, M. K. Oberthaler, R. Schmied, and P. Treutlein, “Quantum metrology with nonclassical states of atomic ensembles,” *Rev. Mod. Phys.*, vol. 90, p. 035005, Sep 2018.
- [13] D. J. Wineland, J. J. Bollinger, W. M. Itano, F. L. Moore, and D. J. Heinzen, “Spin squeezing and reduced quantum noise in spectroscopy,” *Phys. Rev. A*, vol. 46, pp. R6797–R6800, Dec 1992.
- [14] M. Kitagawa and M. Ueda, “Squeezed spin states,” *Phys. Rev. A*, vol. 47, pp. 5138–5143, Jun 1993.
- [15] D. J. Wineland, J. J. Bollinger, W. M. Itano, and D. J. Heinzen, “Squeezed atomic states and projection noise in spectroscopy,” *Phys. Rev. A*, vol. 50, pp. 67–88, Jul 1994.
- [16] J. Ma, X. Wang, C. Sun, and F. Nori, “Quantum spin squeezing,” *Physics Reports*, vol. 509, no. 2, pp. 89 – 165, 2011.
- [17] V. Meyer, M. A. Rowe, D. Kielpinski, C. A. Sackett, W. M. Itano, C. Monroe, and D. J. Wineland, “Experimental demonstration of entanglement-enhanced rotation angle estimation using trapped ions,” *Phys. Rev. Lett.*, vol. 86, pp. 5870–5873, Jun 2001.
- [18] D. Leibfried, M. D. Barrett, T. Schaetz, J. Britton, J. Chiaverini, W. M. Itano, J. D. Jost, C. Langer, and D. J. Wineland, “Toward Heisenberg-limited spectroscopy with multiparticle entangled states,” *Science*, vol. 304, pp. 1476–1478, Jun 2004.
- [19] T. Monz, P. Schindler, J. T. Barreiro, M. Chwalla, D. Nigg, W. A. Coish, M. Harlander, W. Hänsel, M. Hennrich, and R. Blatt, “14-qubit entanglement: Creation and coherence,” *Phys. Rev. Lett.*, vol. 106, p. 130506, Mar 2011.
- [20] T. Takano, M. Fuyama, R. Namiki, and Y. Takahashi, “Spin squeezing of a cold atomic ensemble with the nuclear spin of one-half,” *Phys. Rev. Lett.*, vol. 102, p. 033601, Jan 2009.
- [21] J. Appel, P. J. Windpassinger, D. Oblak, U. B. Hoff, N. Kjaergaard, and E. S. Polzik, “Mesoscopic atomic entanglement for precision measurements beyond the standard quantum limit,” *Proceedings of the National Academy of Sciences*, vol. 106, pp. 10960–10965, Jun 2009.

- [22] I. D. Leroux, M. H. Schleier-Smith, and V. Vuletić, “Implementation of cavity squeezing of a collective atomic spin,” *Phys. Rev. Lett.*, vol. 104, p. 073602, Feb 2010.
- [23] K. C. Cox, G. P. Greve, J. M. Weiner, and J. K. Thompson, “Deterministic squeezed states with collective measurements and feedback,” *Phys. Rev. Lett.*, vol. 116, p. 093602, Mar 2016.
- [24] I. D. Leroux, M. H. Schleier-Smith, and V. Vuletić, “Orientation-dependent entanglement lifetime in a squeezed atomic clock,” *Phys. Rev. Lett.*, vol. 104, p. 250801, Jun 2010.
- [25] J. G. Bohnet, K. C. Cox, M. A. Norcia, J. M. Weiner, Z. Chen, and J. K. Thompson, “Reduced spin measurement back-action for a phase sensitivity ten times beyond the standard quantum limit,” *Nature Photonics*, vol. 8, pp. 731–, Jul 2014.
- [26] O. Hosten, N. J. Engelsen, R. Krishnakumar, and M. A. Kasevich, “Measurement noise 100 times lower than the quantum-projection limit using entangled atoms,” *Nature*, vol. 529, pp. 505–508, Jan 2016.
- [27] B. Braverman, A. Kawasaki, E. Pedrozo-Peña, S. Colombo, C. Shu, Z. Li, E. Mendez, M. Yamoah, L. Salvi, D. Akamatsu, Y. Xiao, and V. Vuletić, “Near-unitary spin squeezing in ^{171}Yb ,” *Phys. Rev. Lett.*, vol. 122, p. 223203, Jun 2019.
- [28] G. Vallet, E. Bookjans, U. Eismann, S. Bilicki, R. L. Targat, and J. Lodewyck, “A noise-immune cavity-assisted non-destructive detection for an optical lattice clock in the quantum regime,” *New Journal of Physics*, vol. 19, p. 083002, Aug 2017.
- [29] D. Meiser, J. Ye, and M. J. Holland, “Spin squeezing in optical lattice clocks via lattice-based QND measurements,” *New Journal of Physics*, vol. 10, p. 073014, Jul 2008.
- [30] J. D. Weinstein, K. Belyov, and A. Derevianko, “Entangling the lattice clock: Towards Heisenberg-limited time-keeping,” *Phys. Rev. A*, vol. 81, p. 030302, Mar 2010.
- [31] L. I. R. Gil, R. Mukherjee, E. M. Bridge, M. P. A. Jones, and T. Pohl, “Spin squeezing in a Rydberg lattice clock,” *Phys. Rev. Lett.*, vol. 112, p. 103601, Mar 2014.
- [32] T. Macrì, A. Smerzi, and L. Pezzè, “Loschmidt echo for quantum metrology,” *Phys. Rev. A*, vol. 94, p. 010102, Jul 2016.
- [33] R. J. Lewis-Swan, M. A. Norcia, J. R. K. Cline, J. K. Thompson, and A. M. Rey, “Robust spin squeezing via photon-mediated interactions on an optical clock transition,” *Phys. Rev. Lett.*, vol. 121, p. 070403, Aug 2018.
- [34] P. He, M. A. Perlin, S. R. Muleady, R. J. Lewis-Swan, R. B. Hutson, J. Ye, and A. M. Rey, “Engineering spin squeezing in a 3D optical lattice with interacting spin-orbit-coupled fermions,” *arXiv e-prints*, p. arXiv:1904.07866, Apr 2019.
- [35] S. F. Huelga, C. Macchiavello, T. Pellizzari, A. K. Ekert, M. B. Plenio, and J. I. Cirac, “Improvement of frequency standards with quantum entanglement,” *Phys. Rev. Lett.*, vol. 79, pp. 3865–3868, Nov 1997.
- [36] I. D. Leroux, N. Scharnhorst, S. Hannig, J. Kramer, L. Pelzer, M. Stepanova, and P. O. Schmidt, “On-line estimation of local oscillator noise and optimisation of servo parameters in atomic clocks,” *Metrologia*, vol. 54, pp. 307–321, Apr 2017.
- [37] B. Braverman, A. Kawasaki, and V. Vuletić, “Impact of non-unitary spin squeezing on atomic clock performance,” *New Journal of Physics*, vol. 20, p. 103019, Oct 2018.
- [38] J. Lodewyck, P. G. Westergaard, A. Lecallier, L. Lorini, and P. Lemonde, “Frequency stability of optical lattice clocks,” *New Journal of Physics*, vol. 13, p. 059501, May 2011.
- [39] H. Levine *et al.*, “Parallel implementation of high-fidelity multi-qubit gates with neutral atoms,” *arXiv e-prints*, p. arXiv:1908.06101, Aug 2019.
- [40] M. A. Norcia, A. W. Young, W. J. Eckner, E. Oelker, J. Ye, and A. M. Kaufman, “Seconds-scale coherence on an optical clock transition in a tweezer array,” *Science*, p. eaay0644, Sep 2019.
- [41] I. S. Madjarov, A. Cooper, A. L. Shaw, J. P. Covey, V. Schkolnik, T. H. Yoon, J. R. Williams, and M. Endres, “An atomic array optical clock with single-atom readout,” *arXiv e-prints*, p. arXiv:1908.05619, Aug 2019.
- [42] S. Sasaki, J. T. Wilson, B. Grinkemeyer, and J. D. Thompson, “Narrow-line cooling and imaging of ytterbium atoms in an optical tweezer array,” *Phys. Rev. Lett.*, vol. 122, p. 143002, Apr 2019.
- [43] J. Borregaard and A. S. Sørensen, “Efficient atomic clocks operated with several atomic ensembles,” *Phys. Rev. Lett.*, vol. 111, p. 090802, Aug 2013.
- [44] T. Rosenband and D. R. Leibrandt, “Exponential scaling of clock stability with atom number,” *arXiv e-prints*, p. arXiv:1303.6357, Mar 2013.
- [45] E. M. Kessler, P. Kómár, M. Bishop, L. Jiang, A. S. Sørensen, J. Ye, and M. D. Lukin, “Heisenberg-limited atom clocks based on entangled qubits,” *Phys. Rev. Lett.*, vol. 112, p. 190403, May 2014.
- [46] D. B. Hume and D. R. Leibrandt, “Probing beyond the laser coherence time in optical clock comparisons,” *Phys. Rev. A*, vol. 93, p. 032138, Mar 2016.
- [47] M. Takamoto, T. Takano, and H. Katori, “Frequency comparison of optical lattice clocks beyond the Dick limit,” *Nature Photonics*, vol. 5, pp. 288–292, Apr 2011.
- [48] M. Schioppo *et al.*, “Ultrastable optical clock with two cold-atom ensembles,” *Nature Photonics*, vol. 11, pp. 48–52, Nov 2016.
- [49] C. W. Chou, D. B. Hume, M. J. Thorpe, D. J. Wineland, and T. Rosenband, “Quantum coherence between two atoms beyond $q = 10^{15}$,” *Phys. Rev. Lett.*, vol. 106, p. 160801, Apr 2011.
- [50] G. J. Dick, “Local oscillator induced instabilities in trapped ion frequency standards,” in *Proceedings of the 19th Annu. Precise Time and Time Interval Meeting, Redondo Beach, 1987*, pp. 133–147, U.S. Naval Observatory, 1888. http://tycho.usno.navy.mil/ptti/1987/Vol%2019_13.pdf.
- [51] A. André, A. S. Sørensen, and M. D. Lukin, “Stability of atomic clocks based on entangled atoms,” *Phys. Rev. Lett.*, vol. 92, p. 230801, Jun 2004.
- [52] A. André, *Nonclassical states of light and atomic ensembles: Generation and new applications*. PhD thesis, Harvard University, Cambridge Massachusetts, May 2005.
- [53] D. G. Matei *et al.*, “1.5 μm lasers with sub-10 mHz linewidth,” *Phys. Rev. Lett.*, vol. 118, p. 263202, Jun 2017.
- [54] Minor deviations result from details of the feedback loop, gain factor and measurement contrast.
- [55] Note that at $T_D < 10^{-3}$ s contributions to the Dick effect from neglected technical high frequency noise at Fourier frequencies $\geq 1 \text{ kHz}$ can become significant compared to the noise sources considered here.

- [56] P. Westergaard, J. Lodewyck, and P. Lemonde, “Minimizing the Dick effect in an optical lattice clock,” *IEEE Transactions on Ultrasonics, Ferroelectrics and Frequency Control*, vol. 57, pp. 623–628, Mar 2010.
- [57] J. Borregaard and A. S. Sørensen, “Near-Heisenberg-limited atomic clocks in the presence of decoherence,” *Phys. Rev. Lett.*, vol. 111, p. 090801, Aug 2013.
- [58] N. Shiga and M. Takeuchi, “Locking the local oscillator phase to the atomic phase via weak measurement,” *New Journal of Physics*, vol. 14, p. 023034, Feb 2012.
- [59] A. Shankar, G. P. Greve, B. Wu, J. K. Thompson, and M. J. Holland, “Continuous real-time tracking of a quantum phase below the standard quantum limit,” *Phys. Rev. Lett.*, vol. 122, p. 233602, Jun 2019.
- [60] R. Kohlhaas, A. Bertoldi, E. Cantin, A. Aspect, A. Landragin, and P. Bouyer, “Phase locking a clock oscillator to a coherent atomic ensemble,” *Physical Review X*, vol. 5, Apr 2015.
- [61] M. Fraas, “An analysis of the stationary operation of atomic clocks,” *Communications in Mathematical Physics*, vol. 348, pp. 363–393, Sep 2016.
- [62] E. Peik, T. Schneider, and C. Tamm, “Laser frequency stabilization to a single ion,” *Journal of Physics B: Atomic, Molecular and Optical Physics*, vol. 39, pp. 145–158, Dec 2005.
- [63] C. W. Gardiner, *Stochastic Methods*, vol. 13 of *Springer Series in Synergetics*. Berlin: Springer-Verlag, 4 ed., 2009.

I. EXPECTATION VALUES AND VARIANCES FOR SPIN SQUEEZED STATES

For $N \gg 1$ (in the simulations starting at $N \geq 20$) we make a Gaussian approximation to the measurement statistics of spin-squeezed states at the end of the Ramsey sequence, meaning that we neglect any cumulants of order 3 or higher in the probability distributions for measurement results of $S_{x,y,z}$. We then only need the expectation values and variances of the collective spin operators and, by construction of the standard Ramsey sequence, S_y and S_x are sufficient. For spin squeezed states generated via the one-axis twisting interaction $e^{-i\frac{\mu}{2}S_z^2}$ these are well known [14]. Due to the finite size of the collective Bloch sphere the contrast of the measurement decays as

$$\frac{\langle S_x \rangle}{S} = \cos^{N-1}(\mu/2) \quad (5)$$

for a system with total spin $S = N/2$. Likewise there is a non-vanishing variance in the polarization direction

$$\frac{\Delta S_x^2}{\langle S_x \rangle^2} = \frac{1}{N} \frac{N(1 - \cos^{2(N-1)}(\mu/2)) - (N/2 - 1/2)A}{\cos^{2N-2}(\mu/2)}. \quad (6)$$

The reduced variance of the squeezed state in the measured direction is

$$\frac{\Delta S_y^2}{\langle S_x \rangle^2} = \frac{1}{N} \frac{1 + \frac{1}{4}(N-1)(A - \sqrt{A^2 + B^2})}{\cos^{2N-2}(\mu/2)} \quad (7)$$

with $A = 1 - \cos^{N-2}(\mu)$, $B = 4 \sin(\mu/2) \cos^{N-2}(\mu/2)$. Note that the reduced variance in this specific spin projection corresponds to ideal alignment of the spin squeezed state with respect to the signal and measurement directions as described in the main text.

Coherent spin states with $\mu = 0$ have the moments

$$\frac{\langle S_x \rangle}{S} = 1, \quad \frac{\Delta S_x^2}{\langle S_x \rangle^2} = 0, \quad \frac{\Delta S_y^2}{\langle S_x \rangle^2} = \frac{1}{N}. \quad (8)$$

In the main text, when discussing squeezed states we always use a squeezing strength $\mu \approx 1.1 N^{-2/3}$ which was independently optimized to give the lowest instability in the dead time free case for each N .

II. OPTIMAL INTERROGATION TIME

In this section we additionally show the optimal Ramsey times corresponding to Fig. 3(c). These are the interrogation times which minimize the model based overall instability, according to Eq. (2), for each N . The results are shown in Fig. 4. Overall they follow the same general trend as the instabilities presented in the main text. This is again due to the fact that in the regime of large particle number and long dead times the instability is limited by

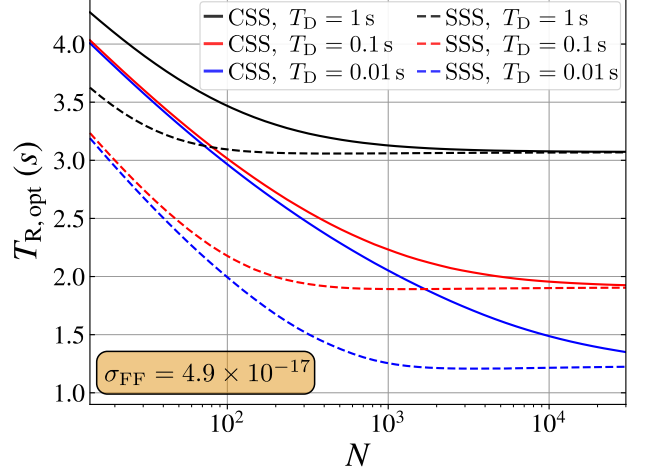


FIG. 4. Optimal Ramsey interrogation times to the results of Figure 3(c) in the main text. Based on the logic of the main text the optimal interrogation times follow the same overall trend as the instability. For the chosen laser noise parameters (see main text for details) they are all on the order of a few seconds.

the tradeoff between Dick effect and CTL which reaches its minimum at an N independent interrogation time. For smaller particle numbers the optimal interrogation time actually depends on N . There, spin squeezed states require reduced Ramsey times compared to the uncorrelated states as the minimum between QPN and CTL shifts to smaller values of T_R when the projection noise is reduced. Again, the optimized squeezing strength here corresponds to weakly squeezed states with the CTL basically unchanged compared to coherent spin states. We further note that for the laser stability assumed here all optimal interrogation times are on the order of a few seconds.

III. STOCHASTIC DIFFERENTIAL EQUATION MODEL

This appendix has the following goals: First, introduce a model for optical atomic clocks based on formulating the time evolution of the stabilized differential phase between laser and atomic reference in terms of a stochastic differential equation (SDE). Then discuss the effects of using a two-stage integrating to correct out local oscillator fluctuations for all noise types considered here. Review how the nonlinear SDE can be approximately solved and thus generate an expression for the resulting clock instability in orders of the phase variances. Finally discuss the onset of fringe-hops and motivate a possible modelling via the mean first passage time.

For the following description we consider an optical atomic clock which operates in repeated, identical cycles of duration T_C . Each cycle contains a Ramsey dark

time $T_R \equiv T$ as well as some dead time $T_D = T_C - T$. Three frequencies are relevant to describe the clock operation: First, the ideal atomic transition frequency ν_0 which we assume is constant for all times. Second, the free-running laser frequency ν_{LO} . For this, the stochastic fractional frequency noise will be described by a noise power spectral density

$$S_y(f) = h_\gamma f^\gamma \quad (9)$$

with $\gamma = -2, -1, 0$ depending on the nature of temporal correlations we wish to study. Third, the stabilized laser frequency ν resulting from the periodic feedback corrections on the free running laser frequency. Now in the following, we discuss the evolution of the stabilized frequency between the Ramsey times of each cycle in order to find an effective measurement variance which describes the long term stability of the clock. The average stabilized frequency difference during the Ramsey dark time of cycle k is

$$\delta\nu_k = \frac{1}{T} \int_{(k-1)T_C}^{(k-1)T_C+T} [\nu(t) - \nu_0] dt \quad (10)$$

and gives rise to a differential phase

$$\phi_k = 2\pi \int_{(k-1)T_C}^{(k-1)T_C+T} [\nu(t) - \nu_0] dt = 2\pi\delta\nu_k T \quad (11)$$

before the measurement at time $(k-1)T_C+T$. Due to the recursive nature of the feedback, the stabilized frequency difference can be split as

$$\delta\nu_k = \delta\nu_k^{LO} - p_{k-1}. \quad (12)$$

The first term, $\delta\nu_k^{LO}$, is the average frequency difference contribution from the free-running laser whereas p_{k-1} is the frequency correction of the servo, applied at the end of the previous cycle. For the differential phase,

$$\phi_k = 2\pi\delta\nu_k T = 2\pi\delta\nu_k^{LO} T - 2\pi p_{k-1} T \quad (13)$$

applies accordingly. The exact form of the correction p_{k-1} depends on the choice of the servo. A frequently used method of feedback is to have an integrator as the servo. In this case, the correction is constructed as

$$p_{k-1} = \frac{g}{2\pi T} \left(\hat{\phi}_{k-1} + \frac{2\pi T}{g} p_{k-2} \right) = \frac{g}{2\pi T} \hat{\phi}_{k-1} + p_{k-2}. \quad (14)$$

Here g is the gain factor and $\hat{\phi}_{k-1}$ an estimator for the accumulated phase during the Ramsey interrogation based on the measurement result (in the simplest case the estimator is just the measurement result itself). From this one finds the coupled stochastic difference equations

$$\delta\nu_k - \delta\nu_{k-1} = \delta\nu_k^{LO} - \delta\nu_{k-1}^{LO} - \frac{g}{2\pi T} \hat{\phi}_{k-1} \quad (15)$$

$$\phi_k - \phi_{k-1} = \phi_k^{LO} - \phi_{k-1}^{LO} - g\hat{\phi}_{k-1} \quad (16)$$

for average frequency and phase. We now focus on the phase equation and the estimate therein, which stems from a measurement outcome of the Ramsey interrogation with either uncorrelated or OAT spin squeezed states. For both cases one finds

$$\begin{aligned} \hat{\phi}_{k-1} = & \frac{\kappa}{T} \sin(\phi_{k-1}) dt + \frac{\kappa}{\sqrt{T}} \frac{\Delta S_x}{\langle S_x \rangle} \sin(\phi_{k-1}) dW_x \\ & + \frac{\kappa}{\sqrt{T}} \frac{\Delta S_y}{\langle S_x \rangle} \cos(\phi_{k-1}) dW_y \end{aligned} \quad (17)$$

where $\kappa = \langle S_x \rangle / S$ quantifies the measurement contrast and $dW_{x,y}$ are Wiener processes for measurement outcomes of $S_{x,y}$ respectively. Here we used the measured phase as the linear estimate of the actual phase value. This form, where formally T could be removed from the first summand, is motivated by our overall goal to develop a stochastic differential equation for the time evolution of the stabilized phase.

As a first result we now show that the single integrator described above is not sufficient to suppress all laser noise types we consider even under otherwise ideal conditions. Especially for stronger temporal correlations, as is the case for random-walk of frequency, this choice of the servo can not fully correct out all fluctuations. This has been a shortcoming in a previous, mathematically more rigorous, approach [61] leading to lower bounds on the stability that can be overcome with a different choice of servo. Modifying the servo is easily possible in the difference equations by adapting the servo correction. Consider now a double-integrator with

$$p_{k-1} = p_{k-2} + \frac{g}{2\pi T} \hat{\phi}_{k-1} + \frac{g_2}{2\pi T} \sum_{n=1}^k \hat{\phi}_{k-n} \quad (18)$$

including longer averages of estimates with the secondary gain factor $g_2 \ll g$. Such secondary integrator stages already find applications in the operation of atomic clocks to also counteract slow drifts of the laser frequency [62]. The effect on the stochastic difference equation is straightforward. To more clearly see the suppression of noise via the double integrator, we transform the finite stochastic difference equations into a system of stochastic differential equations (note that this disregards the dead times now):

$$\dot{\phi} = \dot{\phi}_{LO} - g \frac{\kappa}{T} \phi - g \frac{\kappa}{T^{3/2}} \frac{\Delta S_y}{\langle S_x \rangle} dW_y - \frac{g_2}{T} \psi \quad (19)$$

$$\dot{\psi} = \frac{\kappa}{T} \phi + \frac{\kappa}{T^{3/2}} \frac{\Delta S_y}{\langle S_x \rangle} dW_y \quad (20)$$

where functions of ϕ were expanded only up to linear order and non-linear terms involving products different variables are neglected for now. At this point, we would like to emphasize that neglecting higher orders in ϕ can only be justified for small phase variations. However, if the instability of the atomic clock is to be optimized over

the Ramsey time, these terms must be considered. The increase of instability with T , the coherence time limit (CTL), is substantial for the results of the main text. How this follows from the stochastic differential equation without linear approximation is discussed further below. In addition, the variable $\psi(t)$ was introduced which in general is

$$\begin{aligned}\psi(t) = \int_0^t & \left[\frac{\kappa}{T} \sin(\phi(t')) dt' + \frac{\kappa}{\sqrt{T}} \frac{\Delta S_x}{\langle S_x \rangle} \sin(\phi(t')) dW_x(t') \right. \\ & \left. + \frac{\kappa}{\sqrt{T}} \frac{\Delta S_y}{\langle S_x \rangle} \cos(\phi(t')) dW_y(t') \right].\end{aligned}\quad (21)$$

The system of differential equations can be expressed as

$$\dot{\vec{w}}(t) = M \vec{w}(t) + \vec{f}(t) \quad (22)$$

with

$$\begin{aligned}\vec{w}(t) &= \begin{pmatrix} \phi(t) \\ \psi(t) \end{pmatrix}, \quad M = \begin{pmatrix} -g \frac{\kappa}{T} & \frac{-g_2}{T} \\ \frac{\kappa}{T} & 0 \end{pmatrix}, \\ \vec{f}(t) &= \begin{pmatrix} \dot{\phi}_{LO}(t) - g \frac{\kappa}{T^{3/2}} \frac{\Delta S_y}{\langle S_x \rangle} dW_y(t) \\ \frac{\kappa}{T^{3/2}} \frac{\Delta S_y}{\langle S_x \rangle} dW_y(t) \end{pmatrix}.\end{aligned}\quad (23)$$

Equation (22) can be solved formally via Fourier transform resulting in

$$\vec{w}(\omega) = (i\omega \mathbb{1} - M)^{-1} \vec{g} \quad (24)$$

where

$$\vec{g} = \begin{pmatrix} i\omega \phi_{LO}(\omega) - g \frac{\kappa}{T^{3/2}} \frac{\Delta S_y}{\langle S_x \rangle} dW_y(\omega) \\ \frac{\kappa}{T^{3/2}} \frac{\Delta S_y}{\langle S_x \rangle} dW_y(\omega) \end{pmatrix}. \quad (25)$$

Based on the solution (24) we calculate the spectrum

$$S_w(\omega) = \langle \vec{w}(\omega) \vec{w}^\dagger(\omega) \rangle = (i\omega \mathbb{1} - M)^{-1} \vec{g} \vec{g}^\dagger (-i\omega \mathbb{1} - M^\dagger)^{-1} \quad (26)$$

and find as a part of this the spectrum of the stabilized phase

$$S_\phi(\omega) = \frac{S_{LO}(\omega) + \left[\frac{g_2^2 \kappa^2}{\omega^4 T^5} + \frac{g^2 \kappa^2}{\omega^2 T^3} \right] \frac{\Delta S_y^2}{\langle S_x \rangle^2} S_{dW_y}(\omega)}{1 + (g^2 \kappa^2 - 2g_2 \kappa) / (\omega T)^2 + g_2^2 \kappa^2 / (\omega T)^4} \quad (27)$$

where we used that the laser noise ϕ_{LO} is independent from the atomic measurement results dW_y . In the limit $\omega T / g_2 \ll 1$ this reduces to

$$S_\phi(\omega) = \frac{(\omega T)^4}{g_2^2} S_{LO}(\omega) + \frac{1}{T} \left[1 + \frac{g^2}{g_2^2} (\omega T)^2 \right] \frac{\Delta S_y^2}{\langle S_x \rangle^2} \quad (28)$$

and finally

$$S_\phi(\omega) = \frac{\Delta S_y^2}{T \langle S_x \rangle^2}. \quad (29)$$

These results show first that local oscillator noise is suppressed for all correlations (scalings of the spectral density) considered here, up to $S_{LO}(\omega) \propto 1/\omega^2$, and only the

(white) atomic noise remains. However we note again that this only holds under linear approximation in the stochastic differential equation.

From these results we argue that the double integrating servo completely corrects frequency errors and removes correlations between phases in different measurement cycles. Therefore, we approximate from now on the local oscillator driven phases $d\phi_{LO}$ as uncorrelated Wiener increments with a scaling of the variance $V_\phi = \chi(\gamma) (T_R/Z)^{2+\gamma}$ that is appropriate to the specific noise type within an individual Ramsey dark time, with $\chi = 1, 1.7, 2$ for $\gamma = -1, 0, 1$. Overall, we approximate the stochastic difference equation (16) by the single stochastic differential equation

$$\begin{aligned}d\phi = & \sqrt{V_\phi} d\phi_{LO} - g \frac{\kappa}{T} \sin(\phi) dt - g \frac{\kappa}{\sqrt{T}} \frac{\Delta S_x}{\langle S_x \rangle} \sin(\phi) dW_x \\ & - g \frac{\kappa}{\sqrt{T}} \cos(\phi) \frac{\Delta S_y}{\langle S_x \rangle} dW_y.\end{aligned}\quad (30)$$

An approximate solution to this non-linear SDE can be constructed from a power series ansatz [52]

$$\phi(t) = \sum_{n=1}^{\infty} \epsilon_1^n \phi_{1,n}(t) + \epsilon_2 \sum_{n=0}^{\infty} \epsilon_1^n \phi_{2,n}(t) + \epsilon_3 \sum_{n=0}^{\infty} \epsilon_1^n \phi_{3,n}(t) \quad (31)$$

assuming small perturbation parameters $\epsilon_1 = \sqrt{V_\phi}$, $\epsilon_2 = \frac{\Delta S_y}{\langle S_x \rangle}$ and $\epsilon_3 = \frac{\Delta S_x}{\langle S_x \rangle}$. For details on the further steps and the calculation of the Allan variance in the case of linear feedback we refer to [52] but note that we also included here a term proportional to $\epsilon_2 \epsilon_1^2$ not treated in the reference. The result to lowest orders in the perturbation parameters is

$$\sigma_{\text{eff}}^2(\tau) = \frac{1}{(2\pi\nu_0 T_R)^2} \frac{T_C}{\tau} V_{\text{eff}} \quad (32)$$

with

$$\begin{aligned}V_{\text{eff}} = & \frac{\Delta S_y^2}{\langle S_x \rangle^2} + \frac{\Delta S_x^2}{\langle S_x \rangle^2} V_\phi + \frac{3(1-c)^2}{8} \frac{\Delta S_y^2}{\langle S_x \rangle^2} V_\phi^2 \\ & + \frac{1-3c+8c^2/3}{6} V_\phi^3 + \mathcal{O}(V_\phi^4)\end{aligned}\quad (33)$$

and

$$c = \frac{1}{2} \frac{\langle S_x \rangle}{S} g \quad (34)$$

as applied in the main text.

Finally, it is worth noting that this model, evaluating the Allan variance, often does not correctly reflect the appearance of fringe-hops. Upper limits for safe Ramsey times, within which less than 1 fringe-hop per 10^6 clock cycles occurs, have so far only been determined by numerical simulations of the full stochastic process [36]. According to that study,

$$T_{\text{FH}} = (0.4 - 0.15 N^{-1/3}) Z \quad (35)$$

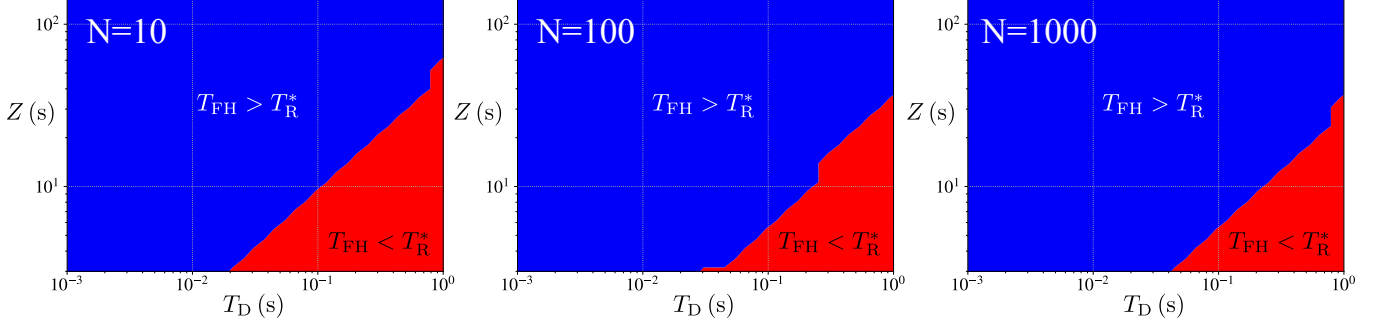


FIG. 5. Comparison between the safe interrogation times T_{FH} (without fringe-hops) and the point of intersection for minimal instability as a function of laser coherence time Z and dead time T_{dead} . Based on this study we can identify regions in which the minimum between Dick effect and CTL can be safely reached (blue) and regions in which additionally the occurrence of fringe-hops has to be investigated in detail (red). By comparing $N = 10, 100$ and 1000 one finds that the red region is largest for small ensembles, short coherence times and larger dead times and decreases in size with increased particle numbers.

and

$$T_{\text{FH}} = (0.4 - 0.25N^{-1/3})Z \quad (36)$$

were suggested as guides for safe interrogation times in the case of flicker frequency and random walk of frequency noise respectively. As described in the main text, this guide can be used to estimate for which parameters fringe-hops may occur before reaching the intersection of Dick effect and CTL. Figure 5 shows corresponding parameter landscapes illustrating the relation of the two time scales, T_{FH} and T_{R}^* , against laser coherence time Z and dead time T_{D} . It can also be seen that the region with $T_{\text{FH}} < T_{\text{R}}^*$ decreases for increasing particle numbers.

In contrast to the numerically motivated guides above, the onset of fringe-hops can also be predicted by further investigations of the SDE as outlined below. This may also allow a better understanding of the underlying processes in the future. First, we observe that the SDE (30) may be expressed more compactly as

$$d\phi = A(\phi)dt + \vec{b}(\phi) \cdot d\vec{W}(t) \quad (37)$$

with

$$A(\phi) = -g\frac{\kappa}{T} \sin(\phi), \quad (38)$$

and the coefficients

$$\vec{b}(\phi) = \left(\sqrt{V_\phi}, -g\frac{\kappa}{\sqrt{T}} \frac{\Delta S_x}{\langle S_x \rangle} \sin(\phi), -g\frac{\kappa}{\sqrt{T}} \cos(\phi) \frac{\Delta S_y}{\langle S_x \rangle} \right)^T \quad (39)$$

to the 3 independent Wiener processes

$$d\vec{W} = (d\phi_{LO}, dW_x, dW_y)^T. \quad (40)$$

Generally, a stochastic differential equation of this form can be rewritten into an equivalent Fokker-Planck equation [63], which in this case reads

$$\partial_t P(\phi, t) = \left[-\partial_\phi A(\phi) + \frac{1}{2} \partial_\phi^2 B(\phi) \right] P(\phi, t) \quad (41)$$

with

$$A(\phi) = -q \sin \phi, \quad B(\phi) = \vec{b} \vec{b}^T = r + s \cos^2 \phi \quad (42)$$

where $q = -g\frac{\kappa}{T}$, $r = V_\phi + g^2 \frac{\kappa^2}{T} \frac{\Delta S_x^2}{\langle S_x \rangle^2}$ and $s = g^2 \frac{\kappa^2}{T} \left(\frac{\Delta S_y^2}{\langle S_x \rangle^2} - \frac{\Delta S_x^2}{\langle S_x \rangle^2} \right)$. The idea for connecting this to fringe-hops is to consider the so-called mean first passage time (mfpt). The mean first passage time describes the average duration over which a random variable (here the stabilized phase) remains within a given interval. Note that the passage time in this cases is again to be regarded as a multiple of the feedback cycle duration. In order to calculate the mfpt we use established tools of stochastic methods [63]. A useful function in the context of mfpt is

$$\begin{aligned} \Psi(x) &= \exp \left\{ \int_0^x dx' \frac{2A(x')}{B(x')} \right\} \\ &= \exp \left\{ \frac{2q}{\sqrt{rs}} \left[\arctan\left(\sqrt{\frac{s}{r}} \cos x\right) - \arctan\left(\sqrt{\frac{s}{r}}\right) \right] \right\}. \end{aligned}$$

From this the mean first time to escape the interval $[-a, a]$, assuming the laser phase starts at $\phi = 0$, is given by [63]

$$T_{\text{mfpt}} = \frac{2 \left[\left(\int_{-a}^0 \frac{dz}{\Psi(z)} \right) \int_0^a \frac{dx}{\Psi(x)} \int_{-a}^x dy \frac{\Psi(y)}{B(y)} - \left(\int_0^a \frac{dz}{\Psi(z)} \right) \int_{-a}^0 \frac{dx}{\Psi(x)} \int_{-a}^x dy \frac{\Psi(y)}{B(y)} \right]}{\int_{-a}^a \frac{dz}{\Psi(z)}}.$$

Which can be further simplified to the double integral

$$T_{\text{mfpt}} = \int_{-a}^a dx \int_{-a}^x dy [2\Theta(x) - 1] \frac{\Psi(y)}{\Psi(x)} \frac{1}{B(y)} \quad (43)$$

where $\Theta(x)$ is the Heaviside function, by using the symmetry $\Psi(x) = \Psi(-x)$.

A maximum Ramsey time T_{FH} without fringe-hops can be specified by requesting that the stabilized phase should not leave the interval $(-\pi, \pi)$ for flicker frequency noise – where it is corrected back to the original reference point – or $(-\pi/2, \pi/2)$ for the more strongly correlated random walk noise, within the simulated $\sim 10^6$ cycles of clock operation. So $T_{\text{mfpt}}(T_{\text{R}}) \leq 10^6$ for $T_{\text{R}} \leq T_{\text{FH}}$, where the functional dependence of the mfpt on T_{R} is based on the parameters q, r, s depending on this quantity. Figure 6 compares T_{FH} as based on the mfpt with results from numerical simulations of the full clock operation as well as the phenomenological guides (35) and (36) in the case of uncorrelated atoms. For both noise types the prediction of the mfpt also exhibits a constant cutoff for large N and reduced T_{FH} for smaller ensembles which is in qualitative and quantitative agreement with the guides and the numerical results. Except the escape interval, as mentioned above, all calculations are without free parameters. For very small ensembles, e.g. $N = 1$, our theory falls short in accurately predicting T_{FH} as it uses the assumption of phases with variance V_ϕ for each interrogation, which in this regime is assumed to break down at larger T_{R} .

IV. NUMERICAL SIMULATIONS

Building on [36] our numerical analysis simulates the closed feedback dynamics of an atomic clock. First, a time series of the laser frequency noise is generated, corresponding to a given noise characteristic. The noise in each cycle, consisting of the mean differential frequency noise $\delta\nu$ in an interval of the measurement duration T_{R} and a further interval of length T_{D} , is generated by discrete stochastic processes. White frequency noise corresponds to independent Gaussian random numbers in each time interval, flicker frequency noise can be generated by a sum of damped random walks, which result in an approximate $1/f$ spectrum over all relevant time scales of the simulation, and random walk of frequency noise results from an ordinary random walk. By specifying a

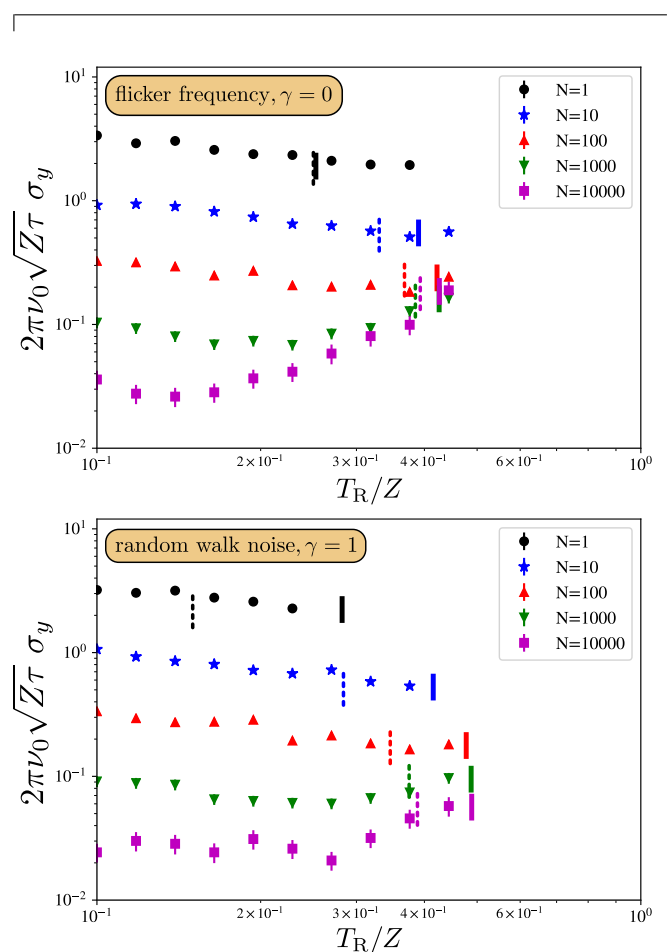


FIG. 6. Numerically simulated clock instability (symbols) for a comparison to the predicted onset of fringe-hops, based on a mean first escape time (solid bars) as well as the safe interrogation times (dashed bars) suggested by Eq. (35) and (36). For both, flicker frequency noise and random walk of frequency noise, we find that the predictions based on the mean first escape time reproduce the observed sudden increase in instability well. To include different noise strengths, we normalized all time scales to the laser coherence time Z (see main text).

noise spectrum with these three correlation types, whose strengths can be characterized by their respective contributions to an Allan variance, a concrete realization of this process is generated as a sum of the individual noise traces. Based on this, the feedback loop can be simulated. For this purpose, a stochastic measurement result of the atomic reference is generated within each interrogation interval according to the differential phase noise $\delta\phi = 2\pi\delta\nu T_{\text{R}}$. For uncorrelated atoms the measure-

ment outcome corresponds to a Binomially distributed random number based on the individual excitation probability $p = \frac{1+\sin(\delta\phi)}{2}$, which is identical for each atom. For spin squeezed states the measurement result is $\mathcal{M} = \langle S_x \rangle / S \left[(1 + \frac{\Delta S_z}{\langle S_x \rangle} \mathcal{N}) \sin(\delta\phi) + \frac{\Delta S_y}{\langle S_x \rangle} \mathcal{N} \cos(\delta\phi) \right]$ where \mathcal{N} are standard-normally distributed random variables with expectation value 0 and variance 1. The measurement results are limited by the fact that their value range may not exceed $-N/2$ to $N/2$ and each result is statistically independent from all others. Using these outcomes the feedback servo generates estimates of the frequency deviations via linear estimation which uses a linear dependence of the measurement result and the phase

or correspondingly the frequency errors from the slope of the signal at $\phi = 0$. Then the feedback corrections are applied using a (double) integrator [36, 62] to stabilize the output frequency. From the stabilized frequency trace the stability at $\tau = 1$ s is extracted by numerically fitting the pre-factor to the asymptotic $1/\sqrt{\tau}$ scaling, reached typically after a few thousand cycles of clock operations in simulations with a total of 8×10^5 cycles. For all simulation results presented in the main text we used moderate feedback with $g = 0.4$ and the squeezing strength was optimized beforehand for each N to give the lowest instability without dead time.